Characteristics of X-Rays

6

In addition to the generation of backscattered and secondary electrons, the interaction of an electron beam with the specimen material releases x-rays which are used to undertake elemental analysis using energy−/wavelength-dispersive x-ray spectroscopy. Characteristics of x-rays are described in this chapter.

6.1   Atom Model

The nuclei of the atoms of specimen material examined in the SEM are composed of protons and neutrons. Since neutrons do not carry a charge, a nucleus is characterized by a concentrated positive charge. The negative charge is carried by electrons that are placed around the nucleus in orbits located at a specific distance. Orbits are grouped together into shells known as K, L, M, etc., each with specific energy defined by the principal quantum number, n. The shells close to the nucleus have the lowest potential energy. Thus, the energy level increases moving away from the nucleus from K to L and M shell. In normal state, the number of electrons in an atom equals the number of protons, and thus an atom does not carry any charge. Electrons occupy shells based on minimum energy. Electrons populate the low-energy shells close to the nucleus before they move onto the higher-energy shells. The negative charge or energy of the electrons is distributed according to their location in orbits. The K shell is closest to the nucleus and is the most tightly bound compared to those (e.g., L or M shells) away from the nucleus. The K shell ($n = 1$, where n is the shell number) is the first shell which is filled in by the electrons followed by L shell ($n = 2$) and so forth. Each shell can hold up to $2n^2$ electrons. Large atoms or heavy elements contain a larger number of electrons and electron orbits.

Each shell is made up of ≥ 1 subshells. The K shell has one subshell "1s"; the L shell has two subshells "2s" and "2p"; the M shell has three subshells "3s," "3p," and "3d"; and so on. Shells are populated according to Pauli exclusion principle which states that only one electron can possess a given set of quantum numbers and that the

© Springer Nature Switzerland AG 2018, Corrected Publication 2023
A. Ul-Hamid, *A Beginners' Guide to Scanning Electron Microscopy*,
https://doi.org/10.1007/978-3-319-98482-7_6

233
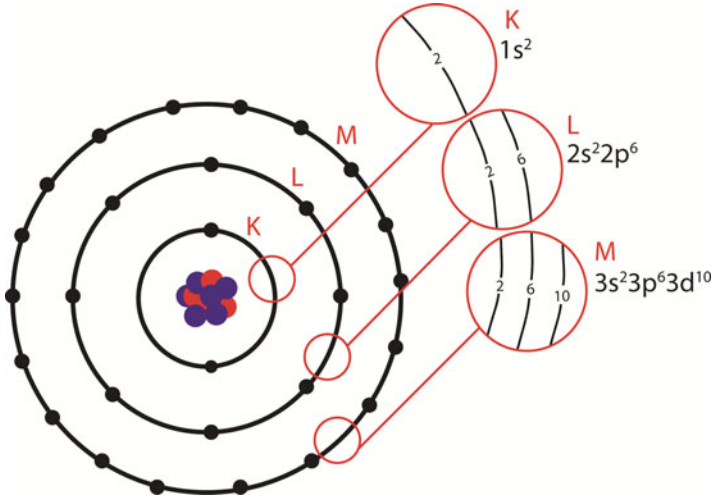
Fig. 6.1 Schematic showing atom model where the maximum numbers of electrons in K, L, and M shells are 2, 8, and 18, respectively

maximum number of electrons in a shell coincides with the number of states possessing the relevant principal quantum number. A subshell is the state defined by azimuthal quantum number "l" within a shell. The values $l = 0, 1, 2, 3$ correspond to s, p, d, and f subshells, respectively. The maximum number of electrons in a subshell is $2(2l + 1)$. This results in 2, 6, 10, and 14 electrons in s, p, d, and f subshells, respectively, as shown in Fig. 6.1.

In x-ray spectroscopy, shells are designated by the letters K, L, M, N, etc. along with their division into subshells. The K shell has no subshell, while L shell contains three subshells (L_I, L_{II}, L_{III}) and M shell contains five subshells (M_I, M_{II}, M_{III}, M_{IV}, M_V). Based on the Pauli exclusion principle, the maximum number of electrons in K shell is 2, in L shell 8, and in M shell 18 as shown in Fig. 6.1.

6.2   Production of X-Rays

6.2.1 Characteristic X-Rays

Primary electron beam penetrates the specimen material and interacts with the inner shells of atoms. As a result, inner-shell electrons of target atoms are ejected from their orbits and leave the bounds of the atom. The process of electron ejection results in a vacancy in the orbital and turns the atom into an ion of excited or energized state. This vacancy is immediately filled when an outer shell electron is transferred to the inner shell, which brings the atom to its ground (lowest energy) state with an accompanying release of energy equal to the difference in the binding energy of the two shells. This excessive energy is released in the form of an x-ray photon (see Fig. 6.2) which has

Incident Electron
(Electron Beam in the SEM)

Scattered Electron

Ejected Orbital
Electron

Electron Transition
(L Shell to K Shell)

X-Ray Photon
Emitted

$E_{X\text{-}ray} = h\nu = E_K - E_L$

$E_{X\text{-}ray}$ = X-ray photon energy
h = Planck`s constant
ν = frequency
E_K = K shell electron energy
E_L = L shell electron energy
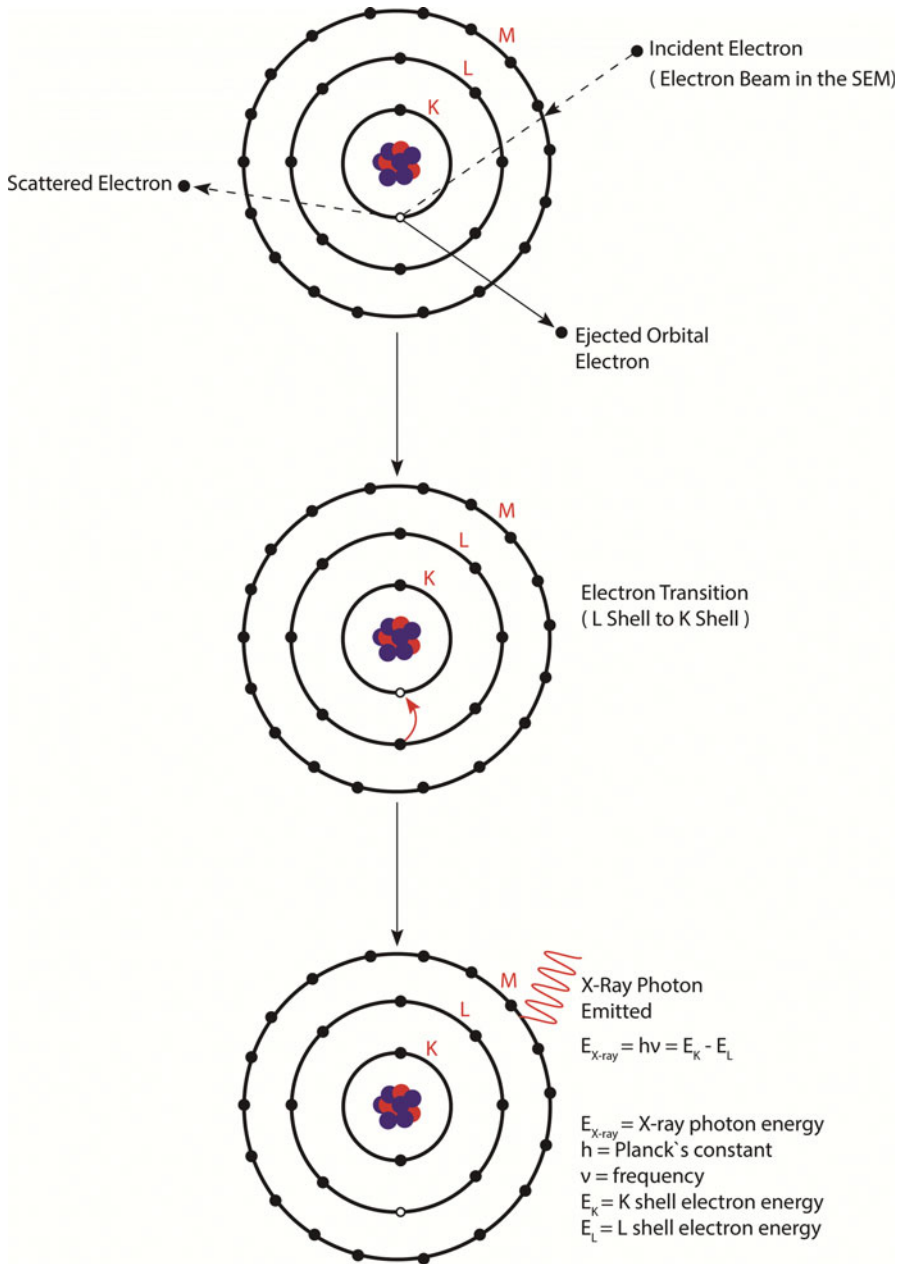
Fig. 6.2 Schematic shows that the electron beam incident upon the specimen knocks an orbital electron out of the K shell. The incident electron is scattered (changes direction and energy), and the knocked out electron is ejected out of the atom into the material. The vacancy created in the k shell is filled up by an electron from the L shell since it has higher potential energy. This is accompanied by the release of a photon whose energy is equal to the difference in the binding energies of the two shells, i.e., E_K–E_L

energy equal to the binding energy between the two shells. For example, if an electron from inner K shell is removed and the vacancy is filled in by an electron from outer L shell, the released x-ray photon will have an energy equal to E_K–E_L where E_K and E_L are binding energies of electrons of K and L shells, respectively. Vacancy produced in L shell is filled in by an electron from M shell giving rise to the emission of another x-ray photon. Large atoms with a large number of electrons and shells can give rise to a large number of x-ray photons resulting in an x-ray spectrum. The incident beam electron is scattered upon collision with the orbital electron changing direction and losing energy that is at least equal to the binding energy of the ejected orbital electron. For instance, in Fig. 6.2, the incident beam electron loses energy corresponding to the energy of the K shell (E_K). On the other hand, ejected orbital electron leaves the atom shell with an energy that varies from a few eV up to few keV depending on the nature of scattering interaction. The excited atom can release its excess energy and attain ground state by another process, i.e., through emission of Auger electron. In this process, the difference in the shell energies is not released as an x-ray photon but is transmitted to another outer shell electron, which then ejects out of the atom with specific kinetic energy.

Each shell around the atom has a specific amount of energy, which is known as the atomic energy level. It represents a characteristic energy of a specific element. Thus, the difference in the energy levels of these electron shells is considered as a characteristic value of an element. Therefore, electron transitions between any two shells result in the release of x-ray photons with an energy unique to an element. These x-ray photons have sharply defined energy values that occupy distinct energy positions in the x-ray spectrum. These x-rays are termed as *characteristic x-ray* lines since they are unique to the element they emanate from. Characteristic x-rays have specific energy depending on the elements that constitute the specimen. Distinct energy positions of x-ray lines form the basis for microchemical analysis where different elements in a specimen material are identified based on their unique orbital transitions.

The production of x-ray photons due to ionization process is known as *fluorescence yield*, which for K shells is higher than that for L shells. In addition, elements with a higher atomic number (e.g., heavy elements) have a higher fluorescent yield (see Fig. 6.3). Low yield for low atomic number (e.g., light) elements is responsible for their low detectability during microchemical analysis. Fluorescent yield for C is as low as 0.001, while for heavy elements it can be close to the value of 1. Fluorescence yield of some common elements is shown in Table 6.1.

6.2.2   Continuous X-Rays

Primary electron beam penetrates the specimen producing not only characteristic x-ray lines as stated above, but it also decelerates (brakes) due to interaction with atomic nuclei which have a positive field of a nucleus surrounded by bonded negative electrons. The energy loss due to deceleration is emitted as a photon of energy:

Fig. 6.3 Plot showing an increase in fluorescence yield with atomic number
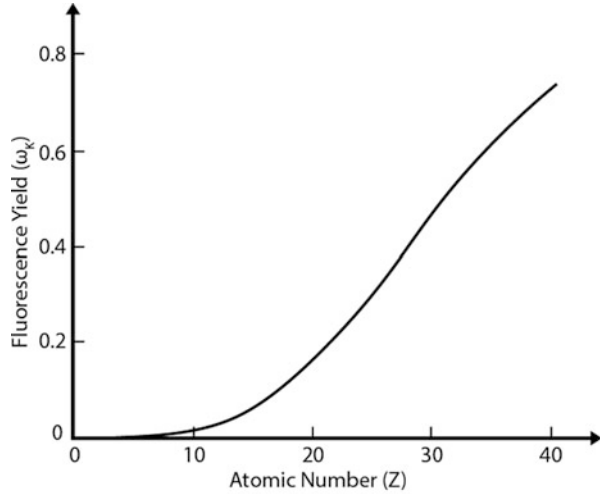
Table 6.1 Fluorescence yield for K_α transition lines of some common elements

Elements	Fluorescence yield for K_α lines
Carbon	0.001
Nitrogen	0.002
Oxygen	0.002
Sodium	0.020
Magnesium	0.030
Aluminum	0.040
Silicon	0.055
Phosphorus	0.070
Sulfur	0.090
Chlorine	0.105
Potassium	0.140
Calcium	0.190
Titanium	0.220
Chromium	0.260
Iron	0.32
Nickel	0.375
Copper	0.410
Zinc	0.435
Tin	0.860

$$\Delta E = h v \tag{6.1}$$

where ΔE is the energy of the emitted photon, h = Planck's constant, and v = frequency of electromagnetic radiation.

The interaction of the incident electron beam with the target atoms is occurring in a random manner; therefore, any electron deceleration may have different energy

losses. Consequently, the continuum x-rays are produced at any value of energy ranging from zero to the maximum energy supplied by incident electrons, thereby forming a continuous electromagnetic spectrum called *continuum* or *white radiation or bremsstrahlung (braking radiation)*. For instance, if the incident electron beam reaches the sample with 20 keV of energy, it will generate continuum x-ray radiation extended from 0 up to 20 keV (see EDS spectrum shown in Fig. 6.4).

Continuum is generated due to all atoms in a specimen and appears as background in an x-ray spectrum. Since it is not unique to a particular element, it is devoid of any unique feature. Background intensity (i.e., continuum x-ray) is larger at the low-energy beam (see Fig. 6.5) and decreases with increasing x-ray energy. Not all of the generated x-rays are detected; some of them are absorbed inside the specimen material or in EDS detector window [1].
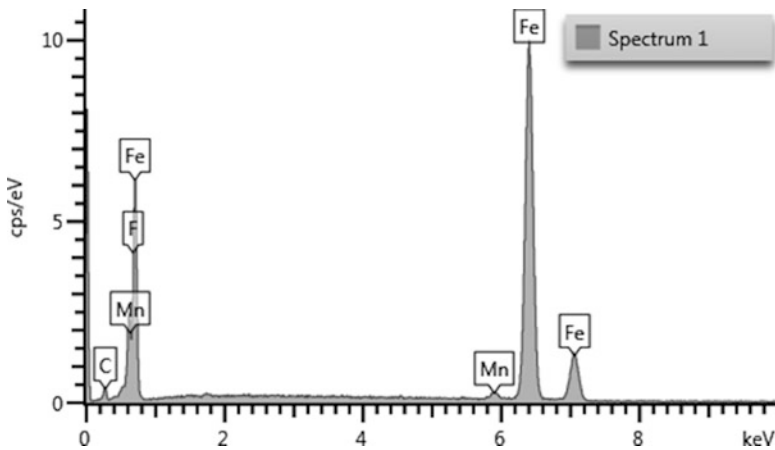
Fig. 6.4 Characteristic x-rays (peaks) and continuum (background) that together make up an energy-dispersive x-ray spectroscopy (EDS) spectrum obtained from a steel sample

Fig. 6.5 Schematic of EDS spectrum showing high background (continuum) at low beam energy
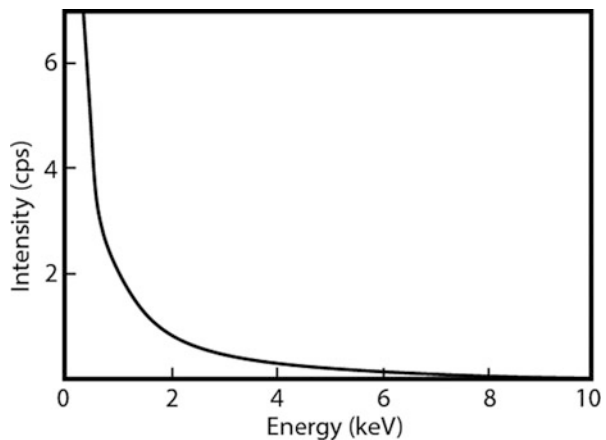
6.2.3 Duane-Hunt Limit

Electron beam energy (E, keV) and wavelength (λ) of x-rays generated from a specimen are bound by the following relationship:

$$\lambda = \frac{1.2398}{E} \tag{6.2}$$

where λ is the wavelength of the x-ray in (nm) and E is the electron beam energy measured in keV. The above equation shows that x-rays with higher energy will have a shorter wavelength. It can be seen in Fig. 6.6 (i) that the highest x-ray photon energy emanates when electron beam loses all of its energy in a single deceleration event. This introduces the concept of x-ray with short-wavelength limit (λ_{SWL}) or minimum wavelength (λ_{min}). It states that x-ray photon of highest energy (or shortest wavelength) is generated when all of the incident beam (E_0) loses its energy instantly and is converted to photon energy. Since the wavelength varies inversely with the energy of the photons, this limit is referred to as short-wavelength limit. It is also called *Duane-Hunt limit* [2].

It can be seen in Fig. 6.7 that for spectra of carbon sample simulated at various beam energies (10, 15, and 20 keV), the Duane-Hunt limit increases with primary beam energy. The point where extrapolation goes to zero is considered the Duane-Hunt limit.

6.2.4 Kramer's Law

The intensity of the continuum x-rays also depends on the atomic number of specimen material as demonstrated by Kramer [3].

$$I_{cm} \approx i_p Z \frac{E_0 - E_v}{E_v} \tag{6.3}$$

where I_{cm} represents x-ray intensity of the continuum background, i_p represents current of the probe, and the average atomic number value is represented by Z, while E_0 is the energy of the incident electron, and E_v is the energy of the continuum photon at a point in the spectrum. It is clear from Eq. 6.3 that the continuum intensity changes proportionally to the average atomic number of the specimen target and that could be explained by high Z targets having more charge. In addition, the intensity of the continuum is increased proportionally with the probe current and the amount of the beam energy. In addition, a significant increase of continuum intensity at the low-energy end of photons (E_v) is observed. This rapid increase in the continuum intensity is due to the higher probability for slight deviations in the trajectory resulting from the Coulombic field of the atoms at low E_v.

(i)

E_0
(Primary Electron Energy)

E_{photon}

Nucleus

Coulombic Field of Atoms

$E_{photon} = h\nu = E_0$ (Primary electron loses all energy in a single event,
Photon energy equals the primary electron energy)

(ii)

E_{photon} E_0
(Primary Electron Energy)

Nucleus

Coulombic Field of Atoms

E_f

$E_f = E_0 - E_i > 0$ (Primary electron loses energy in multiple events)

$E_{photon} = h\nu = E_0 - E_f$ (Photon energy equals the primary electron energy less E_f, where $0 < E_{photon} < E_0$)

(iii)

E_0
(Primary Electron Energy)

Nucleus

Coulombic Field of Atoms

E_f

$E_f = E_0$ (Primary electron loses zero energy, no photon emitted)

Fig. 6.6 Generation of continuous x-rays due to incident beam deceleration within the specimen. The energy of the emitted x-rays depends on the nature of the interaction between the electron beam and specimen atoms. (i) Emitted x-rays will have the highest energy when the incident electrons lose energy instantly in a single scattering event. (ii) When primary beam loses energy in multiple scattering events, the x-ray energy is equal to the energy lost by the incident electron due to scattering. (iii) If the primary beam fails to lose any energy while passing through the sample, no photons will be generated as a continuum is produced due to deceleration of the primary beam in the sample matrix

6.2.5   Implication of Continuous X-Rays

The continuum x-rays represent the background of the spectrum, and the photons of this type of x-rays have no relationship to the sample component. Thus, it is considered a kind of noise. The photons that emanate due to the background

Fig. 6.7 Duane-Hunt limits for simulated spectra of carbon sample at a beam energy of 10, 15, and 20 keV. Duane-Hunt limit increases with beam energy. Duane-Hunt limit marks the end of continuum background, beyond which the continuum does not show any intensity [2]
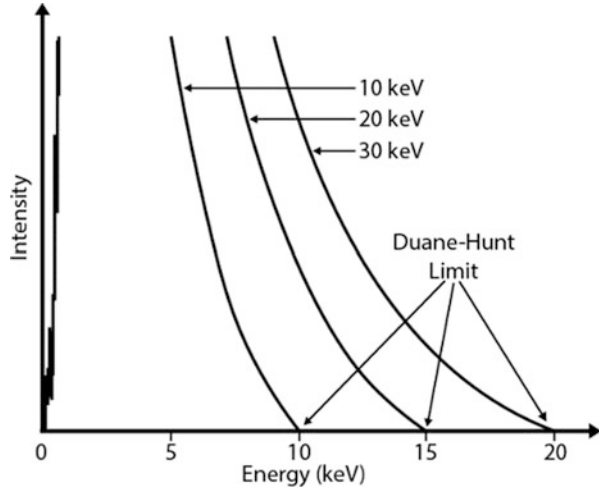
Fig. 6.8 Schematic representation of an EDS spectrum showing characteristic peaks superimposed on background that is formed due to continuous x-rays
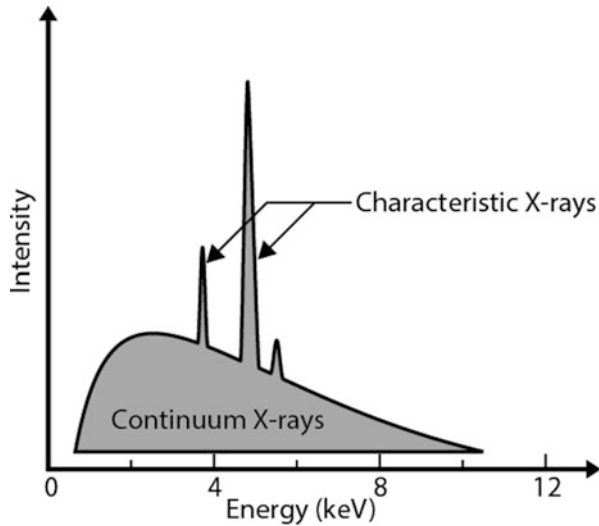
(continuous x-rays) cannot be distinguished from those that originate due to orbital transitions (characteristic x-rays). They both contribute to the x-ray spectrum obtained from a specimen (see Fig. 6.8). Thus, the background present at an energy equal to that of a characteristic x-ray sets a limit to the minimum amount of an element that can be detected using x-ray spectroscopy. Therefore, in order to calculate the concentration of an element, the contribution of background needs to be removed from underneath a characteristic peak.

6.3   Orbital Transitions

6.3.1   Nomenclature Used for Orbital Transition

Energy level diagram represents the energy of electrons in specific shells (see Fig. 6.9). Horizontal lines denote the energy level of an electron state. When the atom is at rest, the case is represented by zero energy. Thus, the atom energy increases upon K, L, M, or N shell ionization. Once the atom returns to the usual level of energy, it emits K_α, L_α, and M_α x-rays. For instance, when an atom is ionized due to the ejection of an electron out of its K shell, the energy of the atom increases by an amount corresponding to the energy of K level. Then, if an electron from L shell travels into the K shell to fill up the created vacancy, the atom energy decreases by an amount corresponding to that of L shell. However, the movement of the electron into the K shell creates a vacancy in the L shell that is required to be filled up by an electron from the M shell level, and so on [1].

Characteristic x-rays are produced due to the transition of electrons between shells. X-ray lines are denoted by the shell from where the electron is originally ejected (i.e., shell of innermost vacancy) such as K, L, M, etc. This is followed by a line group written as α, β, etc. If the transition of electrons is from L to K shell, transition line is designated as K_α. If the transition is from M to K shell, it is designated as K_β. Since the energy difference between K and M is larger than that between K and L, K_β is of higher energy than K_α. Lastly, a number is written to signify the intensity of the line in descending order such as 1,2, etc. Therefore, the most intense K line is written as $K_{\alpha 1}$ and the most intense L line is denoted as $L_{\alpha 1}$. A schematic showing line transitions and their nomenclature is shown in Fig. 6.9. Typical line transitions are also listed in Table 6.2. Not all transitions of electrons between subshells are allowed, thereby resulting in the absence of several lines.

6.3.2   Energy of Orbital Transition

The energy of characteristic x-ray lines varies depending on the type of transitions. For instance, E_K–E_L transitions in a particular element give rise to K_α lines, and E_K–E_M transitions produce K_β lines, which have higher energy. This is followed by E_L–E_M transitions in that element giving rise to L lines. Similarly, E_M–E_N transitions produce M lines with lower energy compared to K and L lines in that particular element. For a given element K, L, M, N, etc., lines will always have different energies and therefore distinct positions in an x-ray spectrum. However, in a multiphase material, different lines from two elements can fall at the same energy position. For instance, M line of a heavy element might overlap with K line of a light element. This means that the energy of x-ray photons emitted due to M transition in a heavy element equals that emitted due to K transition in a light element. Due to the presence of subshells within K, L, M, N, etc., electron jumps (i.e., transitions) also take place within a particular shell.
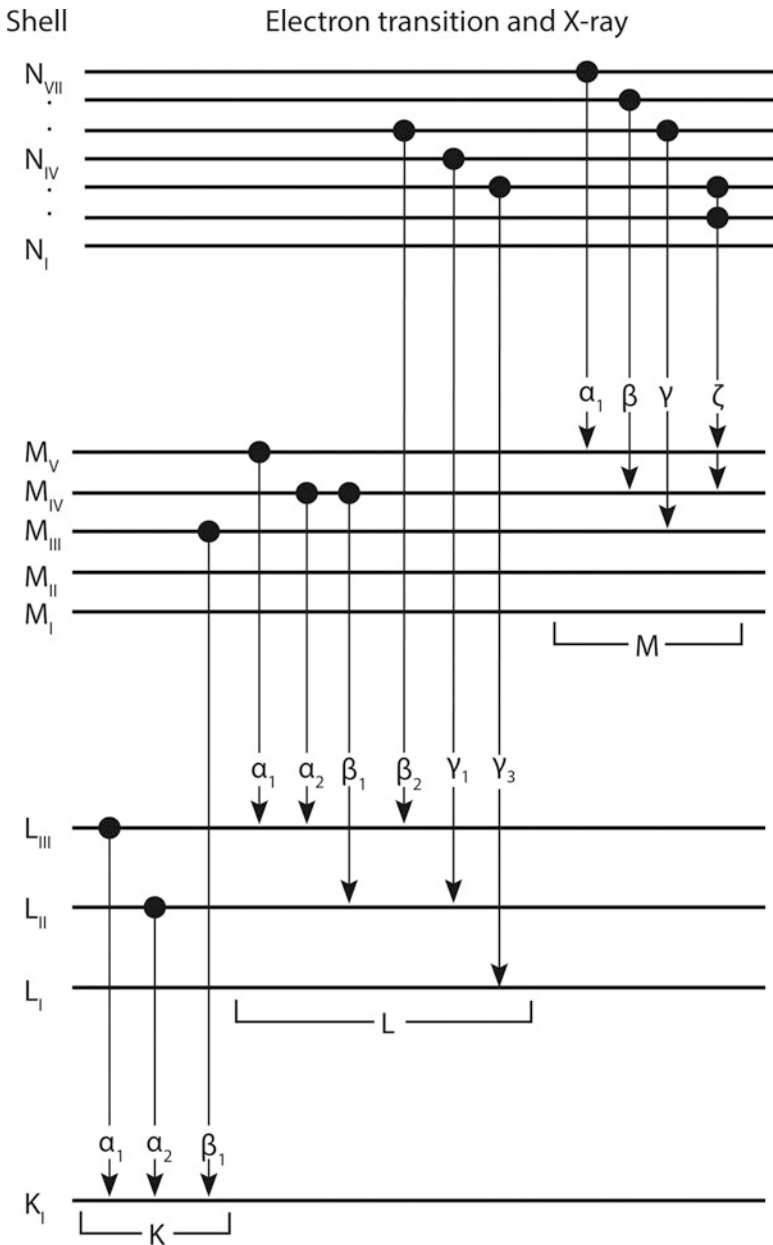
Fig. 6.9 Energy level diagram of an atom showing electron transitions

Transition energy is measured in electron volts (eV); 1 eV of energy corresponds to a change of 1 V in the potential of an electron and equals 1.602×10^{-19} J. Most transition x-ray lines of interest in EDS spectrum fall in the range 1–10 keV. The

Table 6.2 Typical line transitions and nomenclature used

Initial vacancy produced at		
Electron movement from	Electron movement to	X-ray line notation
L_{III}	K	$K_{\alpha 1}$
L_{II}	K	$K_{\alpha 2}$
M_{III}	K	$K_{\beta 1}$
M_V	L_{III}	$L_{\alpha 1}$
M_{IV}	L_{III}	$L_{\alpha 2}$
M_{IV}	L_{II}	$L_{\beta 1}$

total x-ray intensity emanating from a particular shell originates from several transition lines. For instance, for a K shell, >80% of the intensity comes from the $K_{\alpha 1,2}$ line.

6.3.3   Moseley's Law

The energy of a specific atom shell has a unique value that depends on the atomic number (Z) of the material. When x-ray photons are emitted from a material, it has energy characteristic of that atomic number (or material). In 1913, the English physicist Henry Moseley discovered that when the atomic number changes, the energy difference between the shells varies in a regular step. The energy of a photon can be given by Moseley's law below:

$$E = A(Z - C)^2 \tag{6.4}$$

where E is the energy of the x-ray line, Z is atomic number, and A and C are constants with specific values for K, L, M, etc., shells. This forms the basis for identification of elements in materials using x-rays. The above relationship describes energy required to excite any series of transition lines. For instance, x-ray photons of the highest energy in an atom are emitted from K_α shells. This energy equals the binding energy of 1 s electron which in turn is proportional to Z^2 as described above. This energy will be different for each element (depending on its atomic number) and can be used to identify it.

6.3.4   Critical Excitation Energy (Excitation Potential)

The minimum energy required to eject an electron from an atomic shell is known as critical excitation energy or excitation potential (E_c). Since the energy of electrons in a specific shell or subshell is a fixed value, so is the energy required to eject it. As the size of the atom increases (e.g., from light to heavy elements), the energy required to excite any particular transition line also increases. For instance, E_c of Ni K_α is much higher than that of Al K_α. Critical excitation energy of characteristic x-rays for common elements is shown in Table 6.3. The critical excitation energy is also known

Table 6.3 Critical excitation energy of characteristic x-rays for common elements

Critical excitation energy (keV)				
Element	Atomic number	$K_{\alpha 1}$	$L_{\alpha 1}$	$M_{\alpha 1}$ (M_V)
C	6	0.283	–	–
O	8	0.531	–	–
Al	13	1.559	–	–
Si	14	1.838	–	–
Fe	26	7.112	0.709	–
Cu	29	8.979	0.932	–
Mo	42	20.002	2.520	–
Sn	50	29.200	3.929	–
W	74	69.524	10.204	1.809
Au	79	80.723	11.918	2.206
U	92	115.603	17.167	3.552
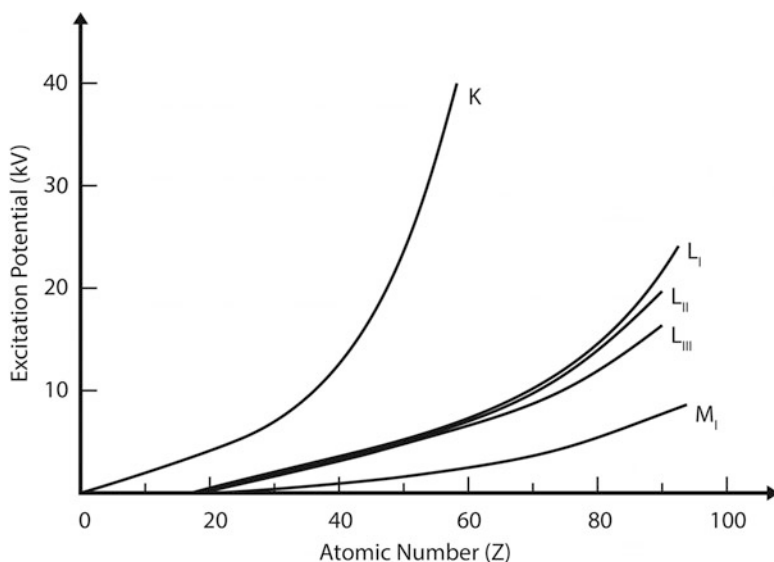
Fig. 6.10 The minimum energy required to eject an electron from an atomic shell (known as excitation potential, E_c) increases with atomic number

as excitation potential, critical ionization energy, and x-ray absorption edge energy. The excitation potential is used to calculate the intensities of characteristic x-rays.

The relationship between excitation potential E_c and atomic number Z for principal shells is shown in Fig. 6.10. It can be seen that E_c increases with Z.

It can be seen in Fig. 6.10 that the excitation potential of K shell is higher than other shells. In addition, the excitation potential of K shell increases extensively with a small increase in the atomic number. While for M_I shell that is located at some distance from the nucleus, the excitation potential is very small compared to the value of K shell for the same atomic number. Its increase with Z is also not

significant. Therefore, the energy required to remove an electron from a specific shell depends on the atomic number of the specimen material.

6.3.5 Cross Section of Inner-Shell Ionization

Cross section of inner-shell ionization (σ or Q) is defined as the probability for an incident beam electron to be inelastically scattered by an atom per unit solid angle Ω. This is represented by the differential scattering cross section as a function of the scattering angle (θ) in Fig. 6.11a. Generally, the inelastic scattering cross section is higher than elastic scattering at low θ but decreases with increasing θ as shown in Fig. 6.11b [4].

The probability of an atom to get excited by the primary electron beam is shown below:

$$Q = \left(\tfrac{1}{E_0 E_c}\right)\log_e\left(\tfrac{E_0}{E_c}\right) \qquad (6.5) \quad [5]$$

where

Q is known as the ionization cross section
E_0 is instantaneous beam energy
E_c is critical excitation energy

The efficiency with which x-rays are generated from an element depends on its fluorescence yield, critical excitation energy for a particular shell (E_c), and primary electron beam energy (E_0). The cross-section values drop as the primary electron energy E_0 increases. In addition, it is lower for elements with the higher atomic number since the critical excitation energy increases with Z.
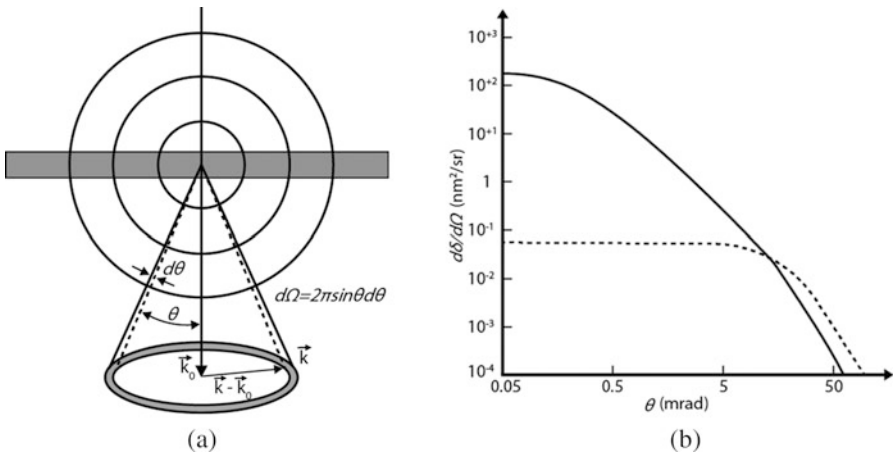
Fig. 6.11 (**a**) Schematic showing the dependence of electron scattering on scattering angle θ. (**b**) Plot showing the angular dependence of the elastic (dashed line) and inelastic (solid line) cross sections for C at 100 kV [4]

Table 6.4 Energy loss due to inelastic scattering [1]

Element	Z	A	ρ (g/cm^3)	J (keV)	dE/ds (keV/cm)	dE/ds (eV/nm)
Carbon	6	12.01	2.1	0.1	2.24×10^4	2.24
Iron	26	55.85	7.87	0.285	6.32×10^4	6.32
Silver	47	107.9	10.5	0.487	6.94×10^4	6.94
Uranium	92	238.03	18.95	0.923	9.27×10^4	9.27

The cross-section of inner-shell ionization depends on the beam energy, which decreases as the beam penetrates further into the sample. The rate of beam electron energy loss (or continuous energy loss approximation) was determined by Bethe in 1930 [6] with the following expression:

$$\frac{dE}{ds}\left(\frac{\text{keV}}{\text{cm}}\right) = -2\pi e^4 N_0 \frac{Z\rho}{AE_i} \ln\left(\frac{1.166E_i}{J}\right) \tag{6.6}$$

$$J(\text{keV}) = \left(9.76Z + 58.5Z^{-0.19}\right) \times 10^{-3} \tag{6.7}$$

where

e is the electron charge ($2\pi e^4 = 1.304 \times 10^{-19}$ for E in keV)

N_0 is Avogadro's number

ρ is the density (g/cm^3)

Z is the atomic number

E_i is the electron energy (keV) at any point in the specimen

A is the atomic weight (g/mole)

J is the average loss in energy per event

The loss of energy is indicated by the negative sign. Bethe's equation had limitations regarding low beam electron energies. These limitations were overcome later by Joy and Luo [7]. Typical values of the rate of energy loss (dE/ds) at 20 keV for various pure elements are shown in Table 6.4 [1].

It is important to determine the values of inner-shell ionization cross section since they have many applications in various fields like materials analysis using electron probe microanalyzer (EPMA) or EDS, thin-film analysis using electron energy loss spectroscopy (EELS), and surface analysis using Auger electron spectroscopy (AES) and in various fields of physics. These values can be determined by theoretical calculations or by experimental work [8].

6.3.6   Overvoltage

Critical excitation energy for a particular shell is approximately equal to the total sum of transition line energies for the outer surrounding shells. For instance, critical excitation energy for U K$_\alpha$ is equal to total line energies of K$_\alpha$ + L$_\alpha$ + M$_\alpha$ (i.e., 98.4 + 13.6 + 3.2 = 115.6 keV) for uranium. The primary electron beam energy must exceed the critical excitation energy (at least twice as much) to enable efficient

excitation. Maximum efficiency is achieved when the primary beam is 2.7 times the critical excitation energy. The relationship of critical excitation energy with primary electron energy is given as follows:

$$U = \frac{E_0}{E_c} \tag{6.8}$$

where

E_0 is the primary energy

E_c is the critical excitation energy

U = Overvoltage

As an example, Fig. 6.12 shows the inner-shell ionization of Si K shell plotted as a function of overvoltage. It can be seen that the inner-shell ionization increases as the overvoltage increases from 1 to 3 followed by a decrease. The latter is attributed to a decrease in the energy of the primary beam due to inelastic scattering within the sample.

As the primary electron beam energy increases, the intensity of a particular x-ray line also increases as shown below [9, 10]:

$$I_c = i_p a \left(\frac{E_0}{E_c} - \frac{E_c}{E_c} \right)^n = i_p a (U - 1)^n \tag{6.9}$$

where

I_c = X-ray line intensity

i_p = Electron probe current

U = Overvoltage

a and n are constants specific for a particular element and shell

The generation of x-rays depends on $(U - 1)^n$ where n varies from 1.3 to 1.6. At small values of U, x-ray generation is minimal as shown in Fig. 6.13.

Fig. 6.12 Inner-shell ionization of Si K shell plotted as a function of overvoltage [1]
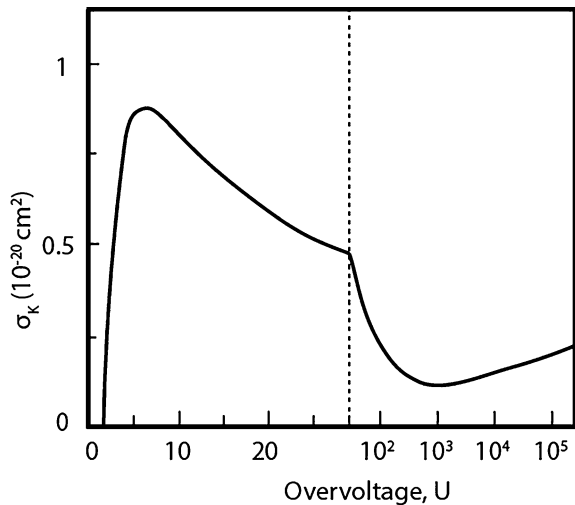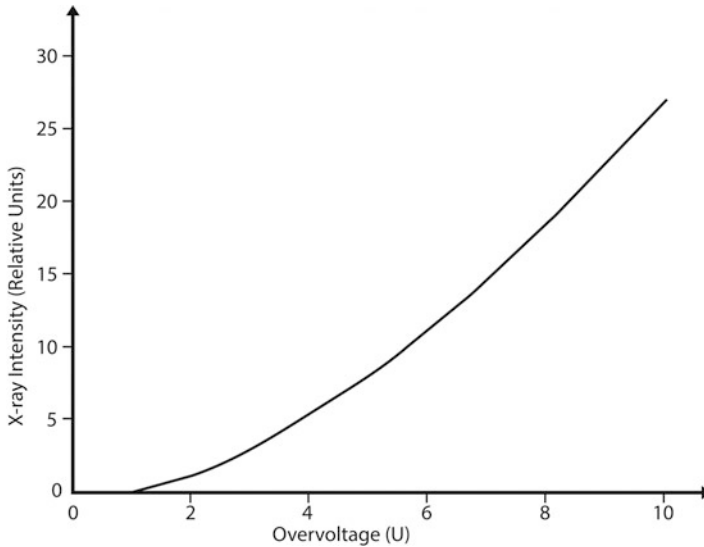
Fig. 6.13 Plot showing a decrease in x-ray generation with decreasing overvoltage, U

6.4 Properties of Emitted X-Rays

6.4.1 Excited X-Ray Lines

Characteristic x-ray peaks are usually very sharp and narrow. For example, the line width of the characteristic peak of calcium is 2 eV only. Because of the thin nature of these peaks, they are referred to in the literature as lines. The width of these lines depends on the resolution of the EDS spectrometer used to plot the spectrum. The width of a peak is typically 70 times wider than the natural width of the line [1].

The number of x-rays emanating from a specimen also depends on the beam current, specimen atomic number, interaction volume, etc. A primary electron beam of 15–20 keV is generally used in the SEM during energy-dispersive x-ray spectroscopy (EDS) to be able to excite characteristic x-ray lines that make detection of most elements possible. For elements with Z >35, an excessively high primary beam energy is required to excite K lines. This is avoided by detecting L and/or M lines (instead of K lines) for heavy elements, which require lesser primary beam energies. Excessively high primary beam energy results in deeper penetration of electron beam and larger interaction volume, which is undesirable in most cases. For light elements, only x-rays of K series are excited, for intermediate elements both K and L series are excited, while for heavy elements L and M series are excited. For a common element such as Zn, most intensely excited x-ray lines are $K_{\alpha 1}$ and $K_{\alpha 2}$ followed by $K_{\beta 1}$, $K_{\beta 2}$, and $K_{\beta 3}$ and then by $L_{\alpha 1}$, $L_{\alpha 2}$, $L_{\beta 1}$, and $L_{\beta 2}$. Series of lines excited for a range of atomic numbers are summarized in Table 6.5.

Table 6.5 Different types of line series excited for a range of atomic numbers

Atomic number	Excited line series
≤ 10	K_α
10–21	K_α, K_β
>21	K_α, K_β, L
≥ 50	L, M

As can be seen from Table 6.5, lighter elements produce a lesser number of lines, while heavier elements produce a large number of lines. Not all transition lines are possible, and the probability of their occurrence varies depending on the atomic number. The greater the difference in energy between two subshells, the lower is the intensity of the x-ray line generated and the less probable its detection. A lot of line transitions possible in theory cannot be seen in the EDS spectrum since they are located too close to other lines and cannot be resolved due to limited energy resolution available in the EDS system.

6.4.2   X-Ray Range

As stated in earlier sections, elastic and inelastic scattering events result in the penetration of electrons into the depth and distribute laterally across the specimen forming a relatively large *interaction volume*. Therefore, the information obtained from the specimen is not restricted to the size of the incident beam but is gathered from a much larger volume. The size of the interaction volume created depends on the specimen density, accelerating voltage of the beam and probe current density. The higher the accelerating voltage, the greater is the depth and the width to which the electrons can travel within the specimen. For specimens with a high atomic number, the elastic scattering is greater which deviates the electrons from their original path more quickly and reduces the distance that they travel into the speci- men. Electron range is defined as the mean straight-line distance of the electron from the point of entry to the point of final rest in the specimen. The path length of an electron trajectory is primarily influenced by and inversely proportional to the atomic number and density of the specimen material for a given beam energy.

X-ray range is the depth of x-ray production within the interaction volume. It mainly depends on the beam energy, the critical excitation energy, and the specimen density. A significant part of the electron range (interaction volume) may produce x-rays depending on the critical excitation energy E_c. Characteristic x-rays are produced within electron range (see Sect. 3.2.6 and Eq. 3.8) for which E_c is exceeded for a particular x-ray line. The range of primary x-ray emission is smaller than electron range. Continuous x-rays are produced due to deceleration of electron beam within the specimen and do not require to surpass E_c for any particular x-ray line. Therefore, white radiation is produced until the electron energy becomes zero. This is shown as a schematic diagram in Fig. 6.14.
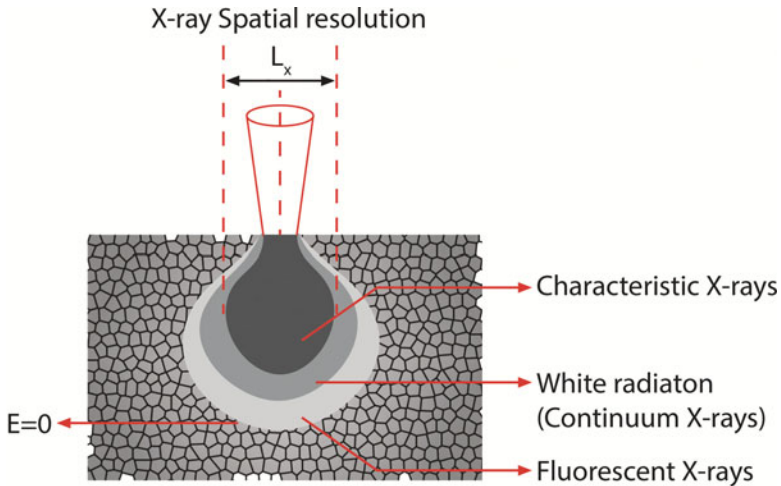
Fig. 6.14 Schematic showing x-ray range which makes up a considerable portion of electron range. Primary beam loses energy at a greater rate as it travels deeper into the specimen material. Characteristic x-rays are produced at depths where critical excitation energy for specimen element(s) is exceeded. Continuous x-rays are produced from greater depths until the primary beam completely loses its energy

X-ray range is given as:

$$R_x = \frac{0.064}{\rho}\left(E_0^{1.68} - E_c^{1.68}\right) \qquad (6.10) \quad [11]$$

where

R_x = X-ray range, microns
ρ = Specimen density, gm/cm^3
E_0 = Incident electron beam energy, keV
E_c = Critical excitation energy, keV

Figure 6.15 shows Cu L$_\alpha$ and Cu K$_\alpha$ in a Cu sample and Al K$_\alpha$ and Cu K$_\alpha$ ranges in an Al specimen as a function of beam energy. It can be seen that electron range is larger than x-ray ranges in Al [11].

6.4.3   X-Ray Spatial Resolution

The depth and width from which x-ray lines are produced depend on the beam accelerating voltage, and atomic number and density of the specimen. X-ray spatial resolution is defined as the maximum width of the interaction volume generated by electrons or x-rays projected up to the specimen surface. Specimens with low atomic number and density allow deeper electron beam penetration and generation of x-ray lines from greater depths. As the depth of penetration increases, so does the lateral diffusion, which degrades the x-ray spatial resolution achieved. Figure 6.16 depicts the electron range and x-ray spatial resolution. It can be seen that materials with low
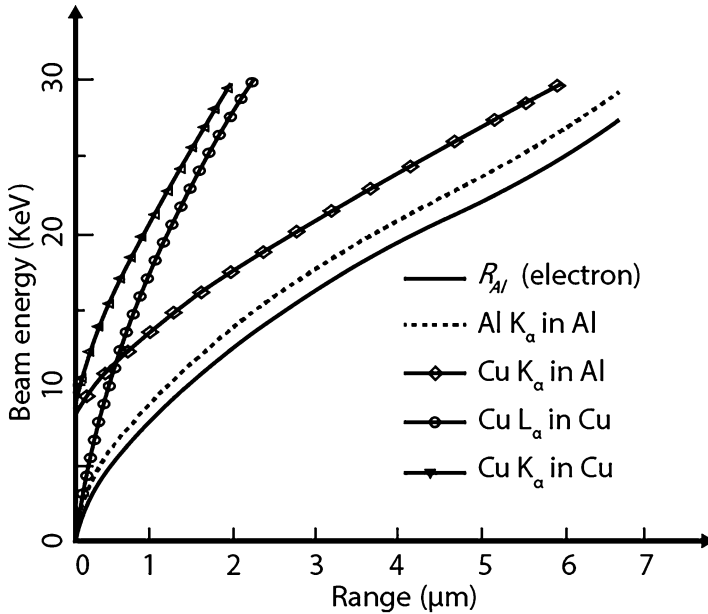
Fig. 6.15 Anderson-Hasler x-ray generation range for Cu L$_\alpha$ and Cu K$_\alpha$ in a Cu sample and Al K$_\alpha$ and Cu K$_\alpha$ ranges in an Al specimen as a function of beam energy. It can be seen that electron range is larger than x-ray ranges in Al [11]
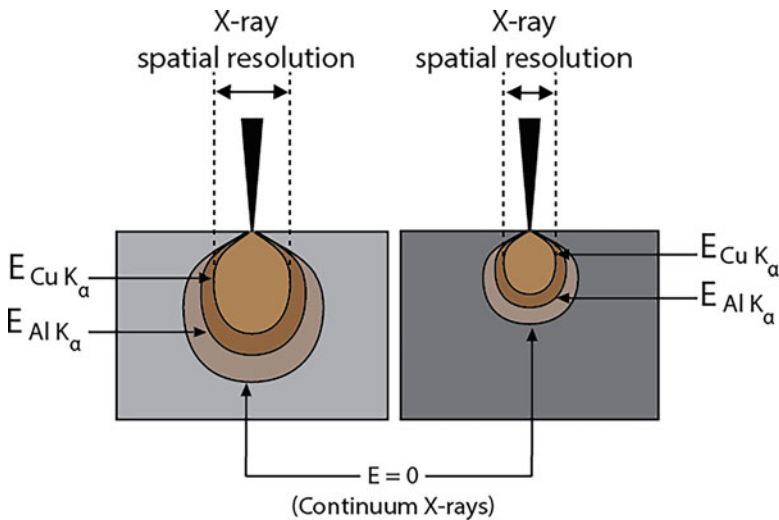
Fig. 6.16 Schematic showing electron range and x-ray spatial resolution for Al-Cu alloy of different compositions at a beam energy of 20 keV. (**a**) Low density 3 g/cm^3 and (**b**) high density 10 g/cm^3. For both Al K$_\alpha$ and Cu K$_\alpha$ x-ray lines, the range of x-ray production is deeper, and the x-ray spatial resolution is wider in the low-density sample than the corresponding range and spatial resolution in the high-density sample. X-rays are generated from a larger volume in low-density material, thus degrading the resolution of x-ray signal (Adapted from [1])

density (low Z) will produce x-ray signals with low spatial resolution as x-rays will be generated from a larger depth and width of the sample.

Higher accelerating voltage reduces the x-ray spatial resolution achieved in a specimen with a thickness typically used in SEM. The shape of interaction volume for the low-density specimen is pear-shaped, while that of a high-density specimen is spherical. X-ray interaction volume also depends on the critical excitation energy of the x-ray line. For example, for the same primary beam energy, the interaction volume for Ni K_α will be different from that for Ni L_α. In addition, x-ray generation within the interaction volume is not uniform and varies along its depth and width. It is higher at the point of penetration of electron beam into the specimen and decreases with distance from that point. It follows that, in order to increase the accuracy and precision of microchemical analysis, the specimen needs to be homogeneous over the entire interaction volume.

6.4.4   Depth Distribution Profile

It is clear from the shape of the sampling volume and Monte Carlo electron trajectories that the distribution of x-ray generation is not uniform both laterally and in depth. The lateral distribution is important for defining the spatial resolution of x-rays. Depth distribution is important because the deeper the generation point of an x-ray, the more distance it has to travel to escape the surface and reach the detector; thus the higher is the probability of the x-ray being absorbed by specimen atoms. Figure 6.17 shows the distribution of x-ray generation points for Al K_α x-rays in pure Al and Cu K_α x-rays in pure Cu, at 10 and 30 keV. On the left-hand side of the figure, there is a histogram of the distribution of generation points with respect to depth. This relation between generation point intensity and depth is called *depth distribution function $\varphi(\rho z)$*. In practice, it is difficult to measure the exact amount of x-ray generated at a certain depth. Therefore, an approximate approach is followed using mass depth, (ρz), method [1]. In general, as the beam energy increases and the atomic number decreases, the sampling volume or the total volume of x-ray generation increases; thus the depth distribution function $\varphi(\rho z)$ is affected.

It can be seen in the histograms in Fig. 6.17 that the depth distribution function is higher directly beneath the surface and decreases to zero as the electron energy becomes less than the critical excitation energy. Nevertheless, we can also see that $\varphi(\rho z)$ becomes higher close to the surface as the atomic number increases with the points of x-ray generation becoming more dense in that area. This is mainly due to two reasons: firstly, as the atomic number increases, the elastic scattering becomes more dominant, and beam electrons get scattered at early stages of sample penetration at a higher probability than for lower atomic number elements. Thus, fewer electrons penetrate to greater depths, and fewer x-rays are generated at those depths. Secondly, as the atomic number increases, critical excitation energy of a particular x-ray line in a sample also increases. The maximum excitation occurs when the electron beam has an overvoltage, i.e., two to three times more energy than the critical excitation energy. So as the critical excitation energy increases, fewer x-rays
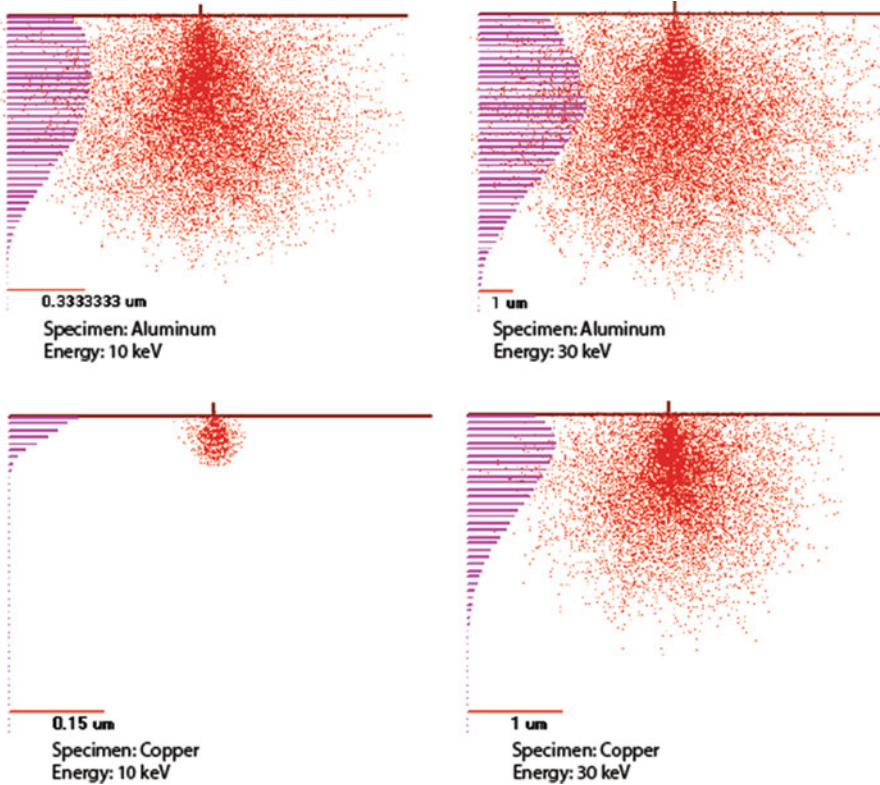
Fig. 6.17 Depth distribution profiles of x-ray generation points for Al and Cu Kα x-rays in pure metals at 10 and 30 keV. Histogram shows the x-ray generation function with mass depth, (ρz). It can be seen that the x-rays are generated from larger vertical and lateral dimensions with an increase in beam energy. The increase is more dramatic in materials with high mass depth (ρz), i.e., Cu. Similarly, the sampling volume is smaller in Cu (high ρz) compared to Al at both beam energies. Moreover, Al has lower critical ionization energy than that of Cu. Therefore, the same primary beam energy generates more x-rays of Al than Cu affecting depth distribution

are being generated, especially at greater depth where beam electrons would have lost much of their energy.

6.4.5   Relationship Between Depth Distribution $\varphi(\rho z)$ and Mass Depth (ρz)

The mass depth (ρz) is the product of the density ρ (g/cm^3) and the linear depth z (cm). The use of the mass depth term ρz is more common than the use of linear depth term z because the mass depth eliminates the need for distinguishing different materials because of their different densities when illustrating the relation with the
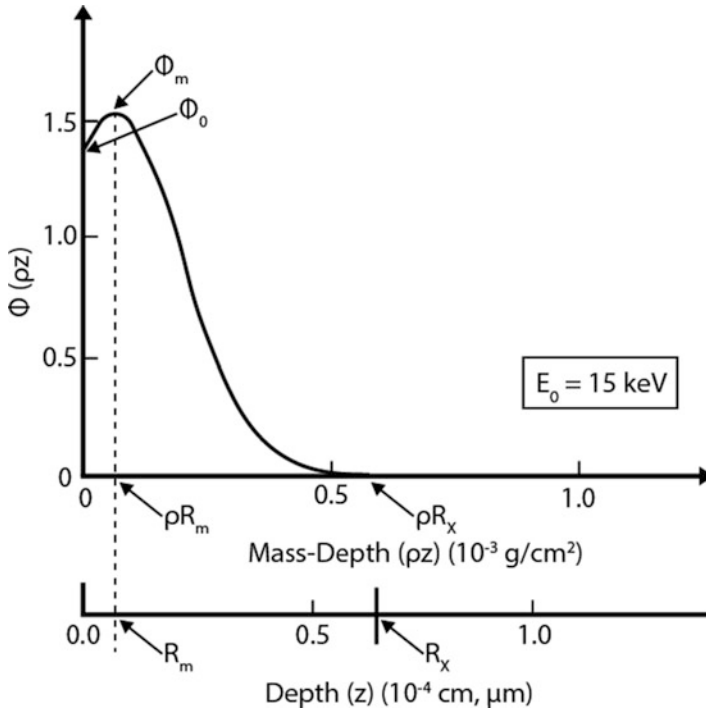
Fig. 6.18 Schematic for the measurement of $\varphi(\rho z)$ curve as a function of ρz and z [1]

depth distribution $\varphi(\rho z)$. Schematic in Fig. 6.18 shows the relationship between depth distribution $\varphi(\rho z)$ and mass depth (ρz).

As an electron penetrates the specimen, it gets scattered or strikes an orbital electron with enough energy to eject it. In the ejection case, the atom will be excited and it will release characteristic x-ray as it de-excites. In the scattering case, either the electron will travel deeper into the specimen, or it will be backscattered. If the electron is backscattered, it will generate x-rays as it leaves the specimen surface. Deeper traveled electron will repeat the scattering process until it is backscattered or its energy becomes lower than the excitation energy.

From the above explanation, we can see that there is a higher probability to generate x-rays near the surface. At greater depths of the specimen, there are fewer electrons because some of them are backscattered, and a lesser number of backscattered electrons is available to generate x-rays compared to the area directly beneath the surface. The generation of x-rays gets a maximum peak at ρR_m. At greater depths, the production of x-ray radiation begins to decrease as the depth increases. This is because the backscattered electrons of the incident beam reduce the number of electrons available at further depths. The electrons that succeed to penetrate deeper lose energy, and therefore they possess less excitation power as they scatter. Finally, x-ray generation points go to zero at $\rho z = \rho R_x$, where the electrons no longer possess an energy that exceeds E_c.

6.4.6 X-Ray Absorption (Mass Absorption Coefficient)

X-rays generated within the specimen target by incident electron beam can—as photons of electromagnetic radiation—undergo absorption by specimen atoms. Three types of x-ray absorption can take place as x-rays travel from their generation point to the detector, namely, elastic scattering, inelastic scattering, and photoelectric absorption.

In elastic scattering, the x-rays are absorbed by electrons of the atom. If the atomic forces—or the ionization energy—are high, the electrons are not ejected; rather, they are forced to oscillate about their mean positions. This oscillation emits a radiation of the same frequency and with no loss of energy in a new direction (Fig. 6.19). This type of scattering is dominant in atoms of high atomic number like gold ($Z_{Au} = 79$) [12, 13].

In inelastic scattering, the x-ray incidents on orbital electrons do not get completely absorbed; rather, part of the x-ray energy is absorbed causing the electron to be ejected with some kinetic energy. The energy loss of the x-ray radiation ΔE is equal to the kinetic energy transferred to the electron as given by the following equation:

$$\Delta E_x = \frac{E_x^2(1 - \cos\theta)}{m_0 c^2 + E_x(1 - \cos\theta)} \cong \frac{E_x^2}{E_0}(1 - \cos\theta) \qquad (6.11)$$

If we take the example of Mo K_α ($E_x = 17.5$ keV) and considering the electron rest energy $E_0 = 511$ keV, we find $\Delta E_x = 600$ eV when $\theta = 90°$. This energy can be detected by an energy-dispersive x-ray detector. This type of scattering dominates in materials with a low atomic number [13].

In photoelectric absorption, photons interact with specimen material in a way that their energy is completely transferred to specimen atoms. In this way, an x-ray photon loses all its energy to an orbital electron, which is ejected with a kinetic energy equal to the difference in photon energy and critical ionization energy required to eject the electron. In photoelectric absorption, either the photon is completely absorbed in a single event, or it continues to propagate without any change in its energy. The intensity of the x-ray radiation—not the energy—will
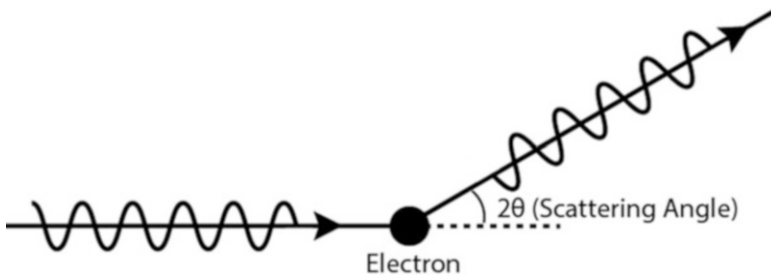
Fig. 6.19 Schematic showing elastic scattering of x-ray
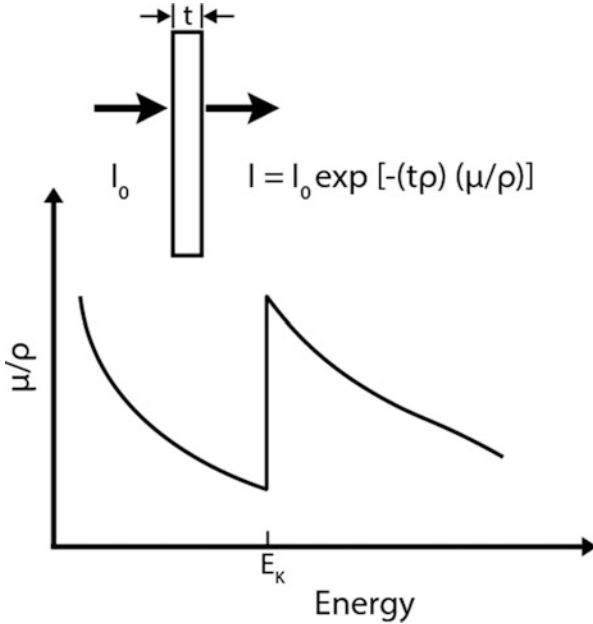
Fig. 6.20 Schematic showing absorption of x-rays and variation of the absorption coefficient with energy. The higher the energy of the x-rays generated within the specimen material, the lower is the mass absorption coefficient, i.e., x-rays will pass through the specimen easily. However, if the x-ray is energetic enough to overcome critical ionization energy and knock out an orbital electron of the constituent element, the mass absorption coefficient increases dramatically, i.e., absorption of x-ray occurs. This is indicated as a sudden increase in the coefficient at E_k in the schematic above. Further increase in x-ray energy will not increase absorption, as the x-ray energy will become too high for proper coupling (between the x-ray and atom) to initiate ejection of the orbital electron [12]

decrease due to photoelectric effect with an exponential decay (see Fig. 6.20) while it travels through a sample, according to the following equation:

$$I = I_0 \exp\left[-\left(\frac{\mu}{\rho}\right)(\rho t)\right] \tag{6.12}$$

where

I is the intensity of x-ray photons when leaving the specimen surface

I_0 is the original intensity of x-ray photons

μ is the absorption coefficient

ρ is the density of the specimen

t is the thickness of specimen traveled

ρt is the area density known also as the mass thickness

$\left(\frac{\mu}{\rho}\right)$ is the mass absorption coefficient of the absorber for the specific x-ray energy, cm^2/g

Absorption takes place by way of ejection of an orbital electron from its respective shell with a transfer of energy from the x-ray photons resulting in their complete absorption. A sharp increase in mass absorption coefficients is observed at energies corresponding to K, L, and M shell energies. These points of strong x-ray absorption are known as *x-ray absorption edges*.

Different materials absorb x-rays to different degrees and are defined by their mass absorption coefficients $\left(\frac{\mu}{\rho}\right)$. Mass absorption coefficient is a measure of how quickly x-ray intensity is lost within a specimen due to absorption. X-rays leaving the specimen at a high takeoff angle (θ) will travel less within the specimen and will be absorbed to a lesser extent compared to those that leave at a small θ after travelling a longer distance within the specimen. The mass absorption coefficient is equal to the absorption coefficient divided by the density. The absorption coefficient has units of inverse length and density has units of mass per volume. Unit of mass absorption coefficient is (length)^2/mass. The SI unit is cm^2/g or m^2/kg.

The probability of absorption is the highest when generated x-ray photons have energy slightly higher than the critical excitation energy of a particular shell of the specimen material or absorber. In other words, high mass absorption occurs when x-ray energy is just above the absorption threshold of the absorbing element. Unlike electron excitation of inner shells, where the maximum excitation occurs when beam electrons have an overvoltage of the order 2–3, the absorption coefficient of x-ray shows a steep increase when the x-ray energy exceeds only slightly above the critical ionization energy. This effect is stronger for x-rays with low energies. At the other extreme, low absorption occurs for high-energy x-rays that are farther away from the absorption threshold [12, 13]. Values of $\left(\frac{\mu}{\rho}\right)$ are widely variable, ranging from <100, for x-rays of high energy and absorbers of low atomic number, to >10,000 for x-rays of low energy and absorbers of high atomic number. In the latter case, severe absorption occurs even for thickness t less than 1 μm [14].

Characteristic x-rays belonging to a particular element (say Ni K$_\alpha$) will always have less energy than critical excitation energy E_c for that element (e.g., for Ni K$_\alpha$). Therefore, a matrix of Ni does not absorb too many of its K$_\alpha$ x-rays. In other words, the mass absorption coefficient of a Ni specimen for Ni K$_\alpha$ will be low. The absorption coefficient of an element for its own radiation is always low because the energy of an element's characteristic radiation is less than the excitation energy of the element. Thus, characteristic radiation of an element passes through it with little absorption.

In another example, the mass absorption coefficient of Cu K$_\alpha$ radiation is highest for cobalt (Co) (see Table 6.6). This is because the energy of Cu K$_\alpha$ is slightly higher than excitation energy E_c for Co. On the other hand, the absorption coefficient is smallest for Cu as an absorber since the energy of Cu K$_\alpha$ is lower than E_c for Cu.

In addition to absorption, some of the x-ray intensity is also lost within the specimen due to inelastic scattering. However, this can be ignored since interaction volume used for microchemical analysis is small. Some of the absorption occurs after x-rays leave the specimen. This absorption takes place in the environment or

Table 6.6 Mass absorption coefficients of Cu K_α for various elements [1]

Element (Z)	X-ray energy, keV		$\left(\frac{\mu}{\rho}\right)$ of Cu K_α in a given element (cm²/g)
	K_α	$E_c = E_K$	
Mn (25)	5.895	6.537	272
Fe (26)	6.4	7.111	306
Co (28)	6.925	7.709	329
Ni (28)	7.472	8.331	49
Cu (29)	8.041	8.980	52

while passing through the x-ray detector window that is usually made of beryllium. Lighter elements with low x-ray energies are absorbed in this manner more readily than heavy elements. For instance, x-rays from light elements such as Li cannot pass through Be window used in EDS detector and therefore cannot be identified or measured. Similarly, if the thickness of Be window is increased, more and more x-rays of elements even heavier than Li will be absorbed.

6.4.6.1 Mass Absorption Coefficient in a Single Element

In order for the photoelectric absorption phenomena to occur, the energy of emitted x-ray has to exceed the critical ionization energy of the electron orbiting in the specific shell. Different shells require different x-rays energies for absorption. The maximum effect of photoelectric absorption occurs when the energy of the emitted x-ray slightly exceeds the critical ionization energy of the electron. This is the energy where it is most probable for the absorption of x-ray to occur. Different sample materials also possess different ionization energies. These factors can be correlated by the expression:

$$\frac{\mu}{\rho} = KZ^4 \left(\frac{1}{E}\right)^3 \tag{6.13}$$

The mass absorption coefficient (μ/ρ) can be used to represent how probable it is for photoelectric absorption phenomena to occur. The higher is the absorption coefficient, the more probable is for absorption to occur. It can be seen from Eq. 6.13, as the energy of the x-ray increases, the mass absorption coefficient decreases. However, a sharp jump in absorption coefficient occurs in the energy region slightly exceeding the critical ionization energy for each shell. We can see that as an example in Fig. 6.21, the energy of incident x-ray versus the absorption coefficient for lanthanum ($Z = 57$) as the absorber material. It can be observed that, generally, there is a smooth decrease in absorption coefficient with some sharp jumps at certain energies. These jumps are the x-ray absorption edges for lanthanum, namely, the K edge at $\approx$38.9 keV, the L edges at $\approx$5.9 keV, and the M edges at $\approx$1.1 keV.
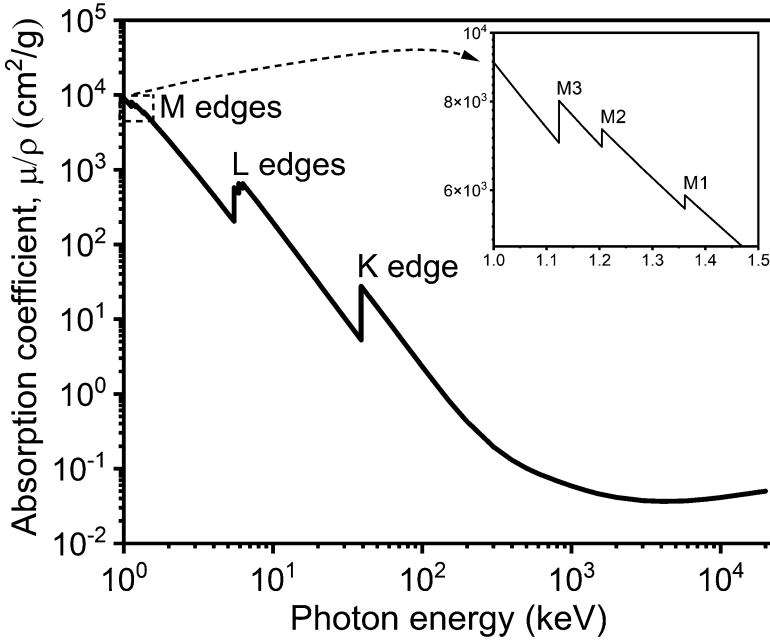
Fig. 6.21 Incident x-ray energy versus mass absorption coefficient in an absorber of lanthanum ($Z = 57$) [1] (plotted with Origin, data from NIST Website for Lanthanum, https://physics.nist.gov/PhysRefData/XrayMassCoef/ElemTab/z57.html)

6.4.6.2 Mass Absorption Coefficient in a Mixer of Elements

The mass absorption coefficient of a specimen containing more than one element is the sum of mass absorption coefficients for each element multiplied by its respective weight fraction. The absorption coefficient can be calculated using the expression:

$$\left(\frac{\mu}{\rho}\right)_{spec}^{A} = \sum_{i} C_i \left(\frac{\mu}{\rho}\right)_{i}^{A} \tag{6.14}$$

where $\left(\frac{\mu}{\rho}\right)_{i}^{A}$ is the mass absorption coefficient for the x-ray energy line from element A passing through element i and C_i is the concentration for each element used in the sample. All elements where absorption is possible to a significant extent should be considered. This consideration is critical, especially for low-energy peaks in the presence of light elements where absorption is important.

For example, in the case of Cu K_α x-ray line passing through a sample of SiO_2, the mass absorption coefficient can be calculated using the following equation:

$$\left(\frac{\mu}{\rho}\right)_{SiO_2}^{CuK_\alpha} = (wt.\text{fraction Si}) \left(\frac{\mu}{\rho}\right)_{Si}^{CuK_\alpha} + (wt.\text{fraction O}) \left(\frac{\mu}{\rho}\right)_{O}^{CuK_\alpha} \tag{6.15}$$

Inserting appropriate values into the equation:

$$\left(\frac{\mu}{\rho}\right)_{SiO_2}^{CuK_\alpha} = (0.468)\left(63.7\frac{cm^2}{g}\right) + (0.533)\left(11.2\frac{cm^2}{g}\right) = 35.8\frac{cm^2}{g}$$

It can be seen that the resultant mass absorption coefficient is affected by both elements' absorption coefficient values and elemental concentration.

As the primary beam energy increases with respect to the critical excitation energy (i.e., E_0–E_c increases), the peak-to-background (P/B) ratio obtained for an x-ray spectrum also increases. This is the ratio of intensities of the characteristic line over the continuum (background). It increases with increasing difference between the beam and critical energies and decreases with increasing atomic number. It is important because it determines the detectability limits of x-ray spectrometer. High P/B ratio has a positive influence on the ability to distinguish or remove continuum background from characteristic x-rays, in order to accurately determine the concentration of a particular element. However, as stated earlier, increasing primary beam energy will also result in its deeper penetration into the material. This will adversely affect the x-ray spatial resolution and increase absorption of x-rays within the specimen material. Absorption is one of the most crucial limiting factors to undertake the accurate microchemical analysis. It reduces the measured x-ray intensity, affects the detectability limits of elements, and necessitates absorption factor corrections during quantitative analysis. Therefore, the optimum value of primary beam energy is not more than two to three times the E_c for a given element. A sample is considered thin if its thickness is small in comparison with the elastic mean free path. It can be approximated using the cross-section of inner-shell ionization. Samples that have a thickness of 100 nm or more are considered thick. The thickness of 10 μm is considered infinite thickness when using SEM electron beam.

6.4.7   Secondary X-Ray Fluorescence

When primary electron beam penetrates a specimen, it ionizes atoms to generate characteristic x-ray photons. These photons, while on their way out of the specimen, may interact with other specimen atoms to cause secondary ionization resulting in the generation of additional characteristic x-rays or Auger electrons. The process by which x-rays are emitted because of interaction with other x-rays is called *secondary x-ray fluorescence* (see Fig. 6.22). Secondary x-rays will have a lower energy than the primary x-ray photons that induce x-ray fluorescence. Both characteristic and continuum x-rays can produce secondary x-ray fluorescence. The energy of the primary x-rays needs to exceed the critical excitation energy of secondary x-ray lines emitted from a particular element in the specimen. Fluorescence is significant only if the primary x-ray energy produced is within 3 keV range of the critical excitation energy of the element producing secondary radiation. The degree of x-ray fluorescence depends on the accelerating voltage, the concentration of the exciting element in the specimen, and the atomic number of the exciting and excited elements [15].

Fluorescence is a consequence of photoelectric absorption effect, and thus, as the mass absorption coefficient of the absorber increases, the fluorescence effect
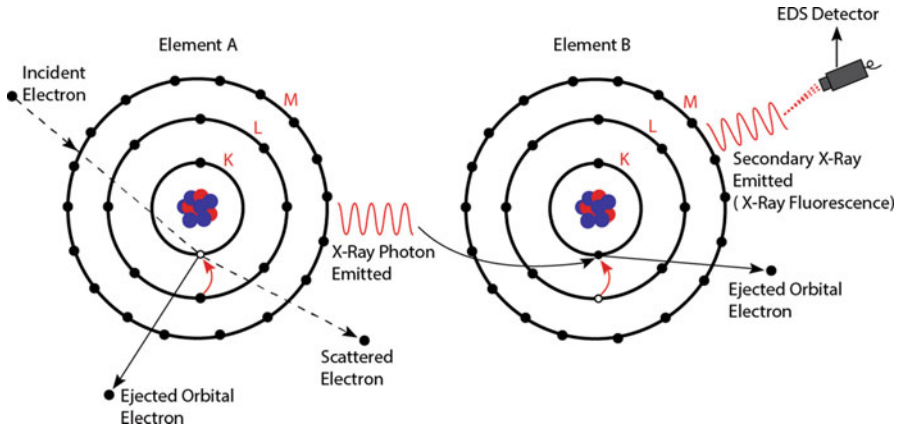
Fig. 6.22 X-ray photons generated by the primary electron beam may interact with other specimen atoms to cause secondary ionization resulting in the emission of additional x-rays. This phenomenon is called *secondary x-ray fluorescence*

Fig. 6.23 Mass absorption coefficient of Ni absorber as a function of x-ray energy. The position of Zn K_α energy line can be seen higher and very close to the critical ionization energy; thus it is strongly absorbed [1] (plotted with Origin, data from NIST Website for Ni and Zn)
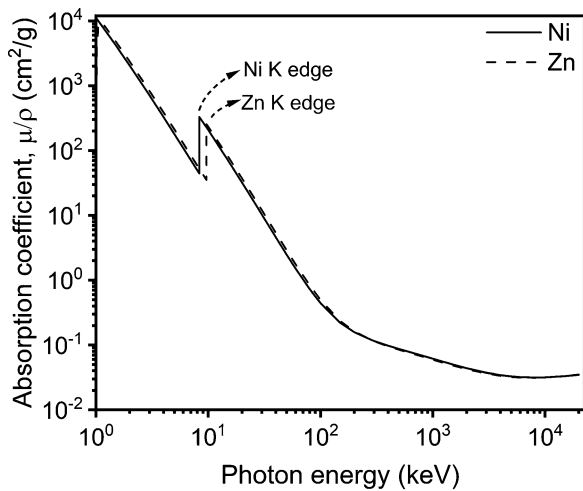
becomes stronger. This can be shown in Fig. 6.23 where the primary radiation is Zn K_α and the absorber is Ni. Nickel K_α fluorescent radiation is produced, as Zn K_α is strongly absorbed by Ni.

The fluorescence effect of different energy lines on a certain element can be estimated by comparing the mass absorption coefficient for each energy line; vice versa, the fluorescence of a certain energy line on different elements can be estimated by comparing different absorption coefficients. For example, Cu K_α line ($E = 8.04$ keV) is strongly absorbed in cobalt ($Z = 27$, $E_c = 7.709$ keV, $\mu/\rho = 326$ cm^2/g), while for nickel, which is only one atomic number higher than cobalt ($Z = 28$, $E_c = 8.331$ keV, $\mu/\rho = 49$ cm^2/g), the absorption coefficient is less

by almost a factor of seven. This is because the energy of Cu K_α line is less than the critical ionization energy of nickel. We can say that the fluorescence effect of Cu K_α in cobalt is much higher than in nickel [1, 12, 14].

Characteristic fluorescence effect occurs in element B purely by characteristic x-ray of element A and not continuum x-ray. For this type of fluorescence to occur, it is necessary that the energy of the characteristic x-ray of element A exceeds the critical ionization energy of element B. For example, the Fe K_α (6.4 keV) can generate characteristic fluorescence of Cr (5.9 keV) x-rays, but not Mn K_α (6.5 keV) lines. However, the Fe K_β (7.0 keV) line can generate Mn K_α x-rays.

The fluorescence effect due to continuum x-rays is referred to as continuum fluorescence, which can take any energy up to the incident beam energy. Therefore, continuum x-rays will always contribute to fluorescence effect if the electron beam has higher energy than the critical ionization energy of the element of interest. However, since the continuum x-rays have a wide range of energies with low intensities, only a small portion of these intensities can cause fluorescence to occur. In practice, the extra intensity of induced characteristic x-ray caused by continuum fluorescence ranges from 1% to 7% for $Z = 20$ to 30 at a beam energy of 20 keV [1].

X-ray fluorescence can complicate quantification of elemental concentrations present within specimen material. For example, in the example cited above, the Zn K_α is strongly absorbed by the Ni specimen to produce Ni K_α fluorescent radiation. This can suppress the primary Zn K_α x-ray line and enhance the Ni K_α line creating a challenge to the accurate measurement of elemental concentration. In another example, the K_α x-ray of Cu element has an energy value of 8.05 keV, and it can be generated by K_α x-ray of Zn that exists in a brass sample. In 70Cu-30Zn alloy, more than expected Cu K_α and less than anticipated Zn K_α x-rays will be generated due to the fluorescence effect. In this way, Cu will be overrepresented, and Zn will be underreported unless corrections are made to the calculations. X-ray fluorescence acquires importance in alloys that have elements with similar Z because it affects the relative amount of characteristic x-rays emanating from compounds. Since x-rays travel farther into the material compared to electrons, the range of x-ray induced fluorescence within the specimen is larger compared to electron-induced range.

References

1. Goldstein J, Lyman CE, Newbury DE, Lifshin E, Echlin P, Sawyer L, Joy DC, Michael JR (2003) Scanning electron microscopy and X-Ray microanalysis, 3rd edn. Springer Science + Business Media, Inc., New York, USA
2. Duane W, Hunt FL (1915) On x-ray wavelengths. Phys Rev 6:166
3. Kramers HA (1923) On the theory of x-ray absorption and of the continuous X-ray spectrum. Phil Mag 46:836. https://doi.org/10.1080/14786442308565244
4. Bell DC, Erdman N (2013) Introduction to the theory and advantages of low voltage Electron microscopy. In: Bell DC, Erdman N (eds) Low voltage electron microscopy: principles and applications. Wiley, UK

5. Green M, Cosslet VE (1961) The efficiency of production of characteristics x-radiation in thick targets by a pure element. Proc Phys Soc 78:1206
6. Bethe H (1930) Zur Theorie des Durchgangs schneller Korpuskularstrahlen durch Materie. Annalen der Physik, Leipzig 397(3):325–400
7. Joy DC, Luo S (1989) An empirical stopping power relationship for low-energy electrons. Scanning 11(4):176–180
8. Llovet X, Powell CJ, Salvat F, Jablonski A (2014) Cross sections for inner-shell ionization by electron impact. J Phys Chem Ref Data 43:013102. https://doi.org/10.1063/1.4832851
9. Green M (1963) In: Pattee HH, Coslett VE, Engstrom A (eds) In proc. 3rd International symposium on x-ray optics and x-ray microanalysis. Academic Press, New York, p 361
10. Lifshin E, Ciccarelli MF, Bolon RB (1980) In: Beaman DR, Ogilvie RE, Wittry DB (eds) In Porc. 8th international conference on x-ray optics and microanalysis. Pendell, Midland, Michigan, p 141
11. Anderson CA, hasler MF (1966) In: Castaing R, Deschamps P, Philibert J (eds) Proc. 4th international conference on X-ray optics and microanalysis. Hermann, Paris, p 310
12. Hawkes P, Spence J (2008) Science of microscopy. Springer, New York
13. Reimer L (1998) Scanning electron microscopy: physics of image formation and microanalysis, 2nd edn. Springer, Berlin
14. Reed S (1993) Electron microprobe analysis and scanning electron microscopy in geology, 2nd edn. Cambridge University Press, Cambridge
15. Wittry DB (1962) Fluorescence by characteristic radiation in electron PRO micro-analyzer, USCEC Report. 84–204. University of Southern California, Los Angeles